A Defect Cluster Model for Ion Migration in Solid Electrolytes

P. G. BRUCE*

Department of Chemistry, University of St. Andrews, St. Andrews, Fife, KY16 9ST, Scotland, United Kingdom

AND I. ABRAHAMS

Department of Chemistry, Heriot-Watt University, Riccarton, Edinburgh, EH14 4AS, Scotland, United Kingdom

A model that describes ion migration in crystalline solid electrolytes in terms of the movement of ion clusters is presented. It is based on investigation of the defect structures of a group of lithium ion conducting solids known as the γ-phases, and of which $Li_{2+2x}Zn_{1-x}GeO_4$ (LISICON) and $Li_{3+x}Ge_x V_{1-x}O_4$ are members. The mobile Li^+ ions in these solid solutions order into defect clusters, which effectively migrate through the solid. $Li_{3+x}Ge_x V_{1-x}O_4$ is one of the best Li^+ ion conductors at room temperature and it is therefore particularly important to understand the mechanism of ion transport in this electrolyte. For both systems the variation of conductivity and defect structure with temperature is correlated, and the general applicability of the cluster model to other nonstoichiometric solid electrolytes, in which solid solution formation occurs entirely within the cation or anion sublattice, is discussed. © 1991 Academic Press, Inc.

Introduction

High ionic conductivity in solids requires a large concentration of mobile species, ions, or vacancies, distributed over an even larger concentration of sites. The sites must also be interconnected by continuous pathways. Beyond these general requirements, several theories have been developed to explain fast ion transport in crystalline solids. It is convenient to differentiate between two classes of solid electrolyte, stoichiometric materials, e.g., α-AgI, and nonstoichiometric solids, e.g., $Zr_{1-x}Ca_xO_{2-x}$.

One of the earliest theories of fast ion

transport was based on the liquid sublattice model, in which the mobile ions were considered to be in a quasimolten state within a rigid framework formed by the immobile lattice (1). This model still finds favor for the description of some stoichiometric solid electrolytes. The second model invokes a random distribution of ions migrating between available sites by thermally activated hopping (2). In its simplest form the model assumes that each mobile species moves independently of the others; however, the model has been developed to include repulsive interactions between the mobile ions (3). The hopping model has been applied to both stoichiometric and nonstoichiometric solid electrolytes. In the case of nonstoi-

chiometric solids the importance of interactions between the mobile species of one sublattice and the charge-compensating ions on the other, has been recognized (4). One example is the association of interstitial F^- ions in $Ca_{1-x}Y_xF_{2+x}$ with the Y^{3+} ions that substitute for Ca^{2+} ions on the immobile cation sublattice, and hence carry an effective charge of $+1$. Clusters form involving several F^- and dopant ions. It has been proposed that these clusters consist of a core containing immobile F^- interstitials and a periphery in which are located mobile F^- interstitials that are nevertheless still bound to the core (5). The dominant feature of this model is the strong association of the interstitial F^- anions with the dopant ions on the cation sublattice.

Recently, we have studied the defect structure of another group of nonstoichiometric solid electrolytes known as the γ-phases, using neutron scattering methods. Two interstitial γ-solid solutions have received particular attention, $Li_{2+2x}Zn_{1-x}GeO_4$ (LISICON) and $Li_{3+x}Ge_xV_{1-x}O_4$ (6–8), the latter system is one of the best Li^+ ion conductors at room temperature yielding values in the range of 10^{-2} Sm^{-1}. These systems also exhibit extensive defect clustering, but unlike the simple fluorites the solid solution mechanism is confined to only one sublattice, in this case that of the cations. We suggest that far from inhibiting ion transport, clustering can enhance it, and describe a possible mechanism of Li^+ ion migration that includes the effective movement of the Li-rich defect clusters through the crystalline solid. To aid comparison between the two γ-solid solutions we concentrate on the $x = 0.5$ composition for each system, i.e., $Li_{3.5}Ge_{0.5}V_{0.5}O_4$ and $Li_3Zn_{0.5}GeO_4$. We begin with a summary of the defect structures of each electrolyte that has previously been determined by neutron diffraction (6–8), then the cluster model of ion transport is described and applied to each system. This is followed by a discussion of the defect structure and the temperature-dependent conductivities. Finally the applicability of cluster migration to other nonstoichiometric solid electrolytes, in which the solid solution mechanism is also confined to either the cation or anion sublattice, is discussed.

Experimental

The conductivities of each solid solution were obtained from a.c. impedance measurements. Sintered disks, some 2 mm thick and 13 mm in diameter were prepared as described previously (9). Gold electrodes were vacuum evaporated onto opposite faces. The disks were mounted in a noninductively wound tube furnace controlled to $\pm 1°C$ and the a.c. measurements were carried out using a Schlumberger Solartron 1255 frequency response analyser and 1286 electrochemical interface under the control of a Zenith personal computer. The electrolyte conductivities were extracted from a.c. impedance plots.

Defect Structures of the γ-Solid Solutions

The detailed description of how the defect structures were determined from neutron diffraction studies is presented in Refs. (6–8). The two lithium ion-conducting solid solutions, which are to be described, are based on the γ-polymorphs of Li_3VO_4 and Li_2ZnGeO_4. The structure of γ-Li_3VO_4 consists essentially of hexagonal close-packed O^{2-} ions with cations in half the tetrahedral sites, ordered in such a way that the VO_4 tetrahedra are isolated from each other and share only corners with LiO_4 tetrahedra. The latter tetrahedra are arranged in groups of three edge sharing sites (Fig. 1). The γ-Li_2ZnGeO_4 structure is identical, with Ge^{4+} ions replacing V^{5+}, and Zn^{2+} ions replacing one-third of the Li^+ ions. The mechanism by which the interstitial, lithium-rich solid solutions form is different for the two γ-
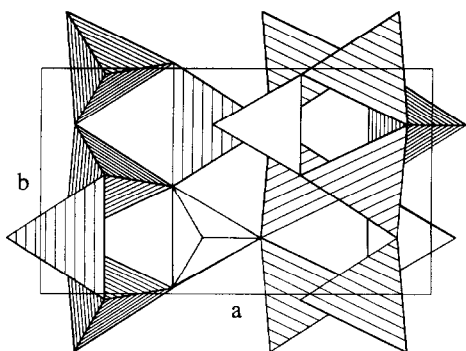
FIG. 1. Unit cell projection onto a/b of γ-Li$_3$VO$_4$ (space group *Pnma*). Open and shaded tetrahedra represent VO$_4$ and LiO$_4$, respectively.

phases. In the case of Li$_{3+x}$Ge$_x$V$_{1-x}$O$_4$ the Ge^{4+} ions substitute directly for V^{5+} and the charge-compensating Li$^+$ ions occupy interstitial octahedral sites. In contrast the formation of Li$_{2+2x}$Zn$_{1-x}$GeO$_4$ involves the substitution of Zn^{2+} by Li$^+$, with the second Li$^+$ ion again occupying an interstitial octahedral site. In both solid solution systems the additional Li$^+$ ions are not randomly distributed over the available octahedral sites and therefore a homogeneous solid solution is not formed. Instead the structure of each solid solution consists of many small regions with the structure of the stoichiometric parent compound and many small regions with the structure(s) of the lithium-rich defect cluster(s). The stoichiometric regions and defect clusters together form a microdomain structure with each region extending by only a few angstroms. For both systems all the interstitial Li$^+$ ions are located in lithium-rich defect clusters; however, the structures of these clusters differ somewhat, and therefore the defect structure of each of the systems is described separately.

Li$_{3.5}$Ge$_{0.5}$V$_{0.5}$O$_4$

At 25°C the solid solution consists of two substructures, one with the structure of stoi-

chiometric Li$_3$VO$_4$ and the other a lithium-rich cluster, the structure of which is shown in Fig. 2(a). The structure of this cluster and the stoichiometric regions differ in that the former contains two octahedrally coordinated interstitial Li$^+$ ions, the sites of which are designated (3) and (4) in Fig. 2(a). Li(3) shares faces with two tetrahedral sites, which are occupied by Li$^+$ ions in stoichiometric Li$_3$VO$_4$, these Li$^+$ ions being displaced into the tetrahedral sites, designated (2a), in the lithium cluster. In fact the displaced Li$^+$ ions are located close to the common face shared between the (2) and (2a) tetrahedral sites. Li(4) shares faces with four tetrahedral sites of which only three are occupied by Li$^+$ ions.

At elevated temperature, 300°C, it appears that two lithium-rich clusters coexist with the stoichiometric structure. One cluster is identical to that at room temperature while the other consists of a Li$^+$ ion in the octahedral site, (4), surrounded by three Li$^+$ ions in tetrahedral sites and one vacant tetrahedral site (2) whose Li$^+$ ion has been displaced into site (2a), Fig. 2(b).

Li$_3$Zn$_{0.5}$GeO$_4$

At 25°C three ordered substructures have been identified; regions with the structure of stoichiometric Li$_2$ZnGeO$_4$ coexist with two lithium-rich defect clusters (Fig. 3(a)). The simplest cluster, which has been designated type I, consists of a Li$^+$ ion in an interstitial octahedral site, (3), sharing two faces with tetrahedral sites, only one of which is occupied by a Li$^+$ ion. In stoichiometric Li$_2$ZnGeO$_4$ the octahedral site is empty and both the face-sharing tetrahedral sites are occupied; it is the presence of Li(3) in the cluster that displaces one of the tetrahedrally coordinated Li$^+$ ions into the neighboring tetrahedral site (2a). The displaced Li$^+$ ion is located close to the common face and between the (2) and (2a) sites. The type II cluster consists of two type I clusters linked via their empty tetrahedral
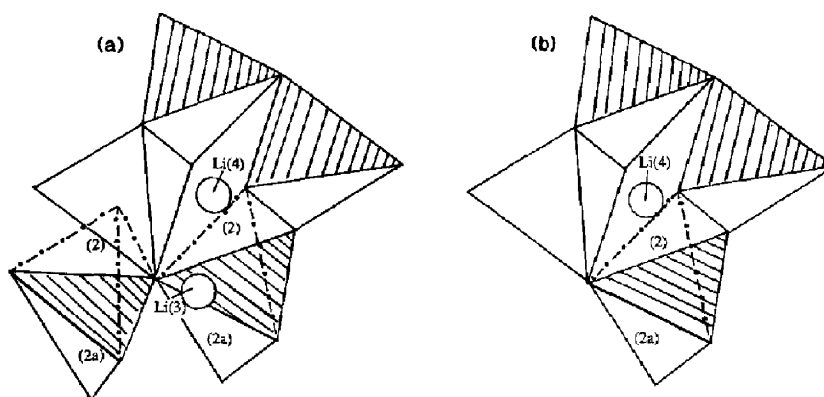
FIG. 2. (a) Lithium-rich defect cluster present at room temperature and (b) additional lithium-rich cluster present at elevated temperature, in $Li_{3.5}Ge_{0.5}V_{0.5}O_4$. In both cases tetrahedra constructed with solid lines represent sites occupied by Li^+ ions, whereas those constructed with chain lines represent sites from which Li^+ ions have been displaced as a result of solid solution formation. Circles represent interstitial, octahedrally coordinated Li^+ ions. Site labels are indicated on the diagrams.
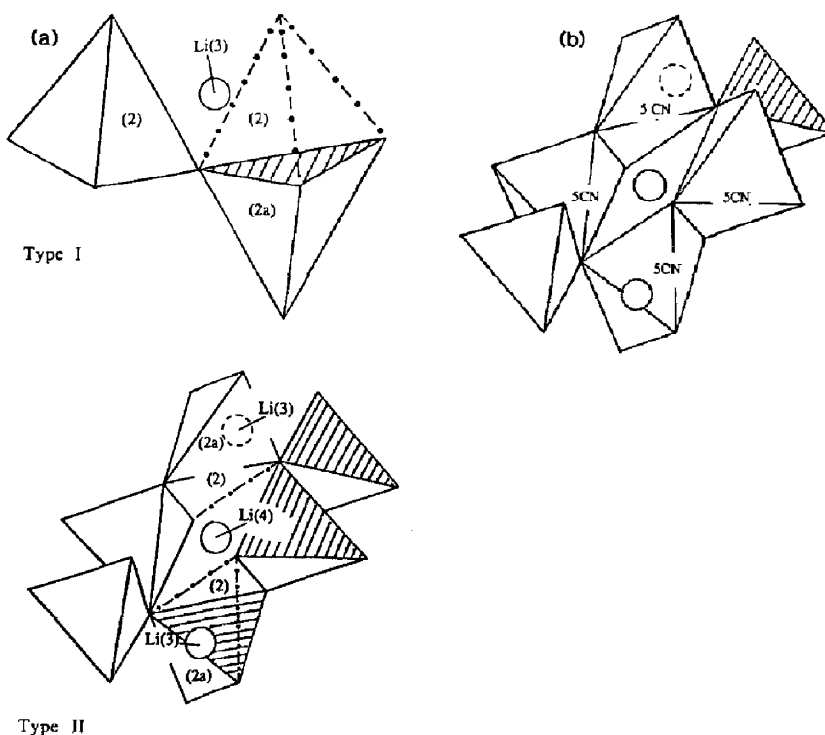

FIG. 3. (a) Types I and II lithium-rich defect clusters present at room temperature and (b) type III cluster present at elevated temperature, in $Li_3Zn_{0.5}GeO_4$. The tetrahedral sites and octahedrally coordinated Li^+ ions are represented as described in Fig. 2. Five coordinate sites containing Li^+ ions are designated 5CN in (b).
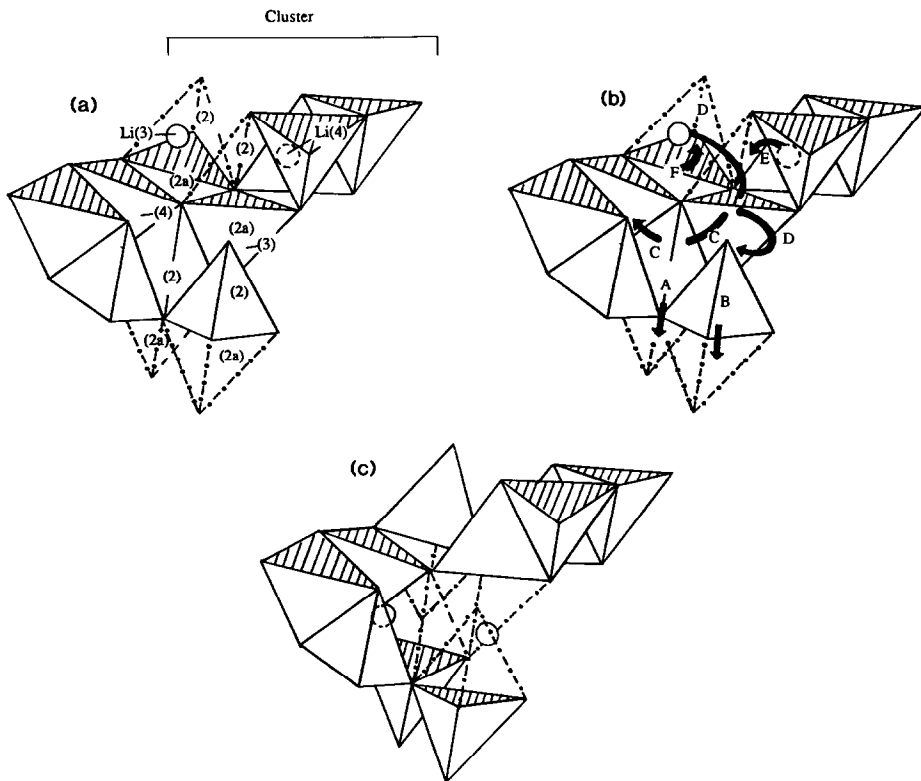
FIG. 4. Mechanism of Li^+ ion transport in $Li_{3.5}Ge_{0.5}V_{0.5}O_4$ by cluster migration, (a) before migration, (b) migration pathways, and (c) after migration. Solid and dashed circles represent visible and eclipsed octahedrally coordinated Li^+ ions. Tetrahedra constructed with solid and chain lines represent respectively occupied and unoccupied Li^+ sites. Arrows in (b) indicate the displacements of each of the Li^+ ions in the cluster.

sites by a central site (4), occupied by Li^+ (Fig. (3a)). The octahedral site (4) shares faces with four tetrahedral sites; two are occupied by Li^+ ions while the two remaining sites are empty. Again the displaced Li^+ ions are located close to the common face between the (2) and (2a) sites.

At temperatures in excess of 300°C, only two substructures are present, viz., the stoichiometric structure and a type III defect cluster (Fig. 3(b)). This new cluster is very similar to the type II cluster but is distinguished by the fact that the two Li^+ ions in the tetrahedral (1) sites, which each share a common face with site (4), are now dis-

placed toward a position close to the common face between the (1) and (1a) sites. In this case all four Li^+ ions around the octahedral site (4) are best regarded as occupying 5-coordinate positions formed by the pairs of tetrahedral sites.

The Cluster Model of Ion Migration

Despite the rather complex nature of the defect clustering present in the two solid solution systems, the essential features of the mobile cluster model of ion transport are common to both systems.
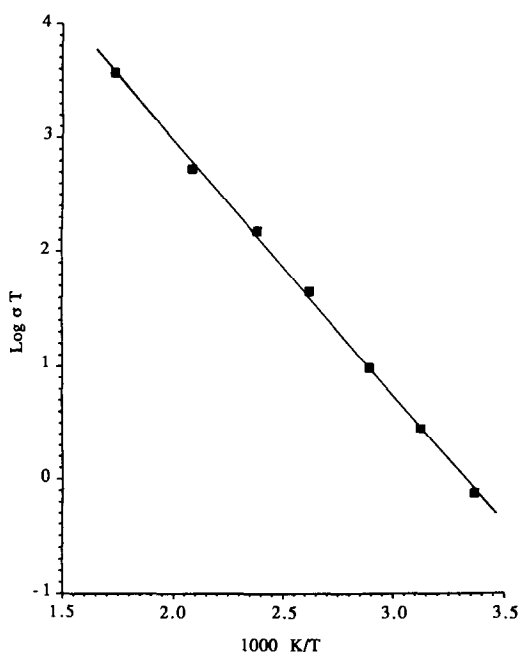
For both γ-phases it is the interstitial solid

FIG. 5. Arrhenius plot for $Li_{3.5}Ge_{0.5}V_{0.5}O_4$ (σ in Sm^{-1}).

solutions that give rise to the high ionic conductivity; stoichiometric Li_3VO_4 and $Li_2Zn GeO_4$ and vacancy solid solutions do not conduct to any significant extent (10). In contrast, the interstitial solid solutions exhibit very high ionic conductivity. For example, $Li_{3.5}Ge_{0.5}V_{0.5}O_4$ possesses a conductivity of approximately 10 Sm^{-1} at 300°C; yet the interstitial ions are not randomly distributed over a set of sites but are contained within ordered clusters of Li^+ ions, the entire structure of the solid consisting of a mosaic of ordered substructures. It does not seem likely that the ionic conductivity is due to a few free Li^+ ions migrating in a random manner in such a highly ordered system. It is in fact possible to describe Li^+ ion transport in these systems without the need to postulate that a proportion of the clusters must decompose to yield some free Li^+ interstitials. Instead the entire lithium-rich cluster can effectively migrate by a con-

certed movement of the Li^+ ions within the cluster; in this fashion, clusters exchange places with stoichiometric regions as the Li^+ ions migrate through the crystal. By comparing the structure of a lithium-rich defect with that of a neighboring stoichiometric region and by taking account of the repulsions between Li^+ ions in face-sharing sites within the cluster, it is possible to postulate mechanisms by which the Li^+ ions in the cluster may undergo cooperative displacements and thus migrate. We have identified what appears to be the simplest mechanism of Li^+ ion migration for both the $Li_{3.5}Ge_{0.5}V_{0.5}O_4$ and $Li_3Zn_{0.5}GeO_4$ electrolytes. Presentation of these mechanisms allows a more detailed appreciation of the conduction process. We first consider the lithium germanium vanadate.

$Li_{3.5}Ge_{0.5}V_{0.5}O_4$

Part of the room temperature structure of $Li_{3.5}Ge_{0.5}V_{0.5}O_4$ comprising a defect cluster and a neighboring region with the stoichiometric structure is shown in Fig. 4. The structure before cluster migration is shown in Fig. 4(a) along with site labels. The pathways followed by each of the migrating Li^+ ions is indicated by separately labeled arrows in Fig. 4(b), and the structure after migration is shown in Fig. 4(c). The displacements of the Li^+ ions shown in Fig. 4(b) may be summarized as follows. Two Li^+ ions in tetrahedral sites (2) are displaced into face-sharing (2a) sites (arrows A and B). A Li^+ ion originally occupying a (2a) site moves into a face-sharing octahedral site (3) then through a site (2) into an octahedral site (4) (arrow C). One of the octahedrally coordinated Li^+ ions moves through a (2) and (2a) site into a new octahedral site (3) (arrow D) and the other octahedral Li^+ ion migrates through a face to occupy a tetrahedral site (2) (arrow E). Finally a tetrahedrally coordinated Li^+ ion in site (2a) is displaced into site (2) (arrow F).

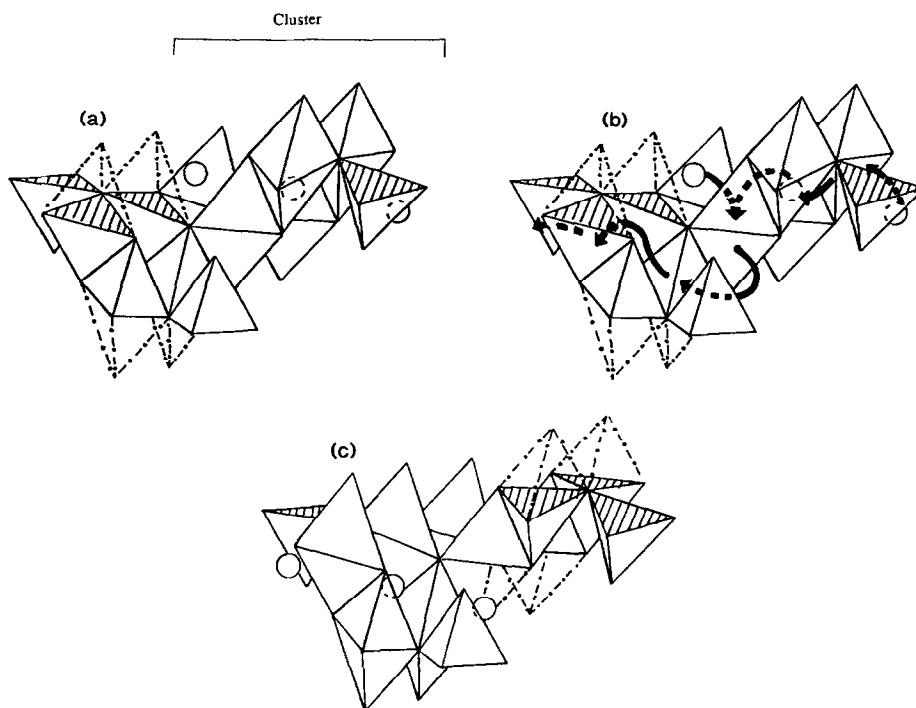Since ion migration is not confined to the

FIG. 6. Mechanism of Li^+ ion transport in $Li_3Zn_{0.5}GeO_4$ by cluster migration, (a) before migration, (b) migration pathway (c) after migration. Solid and dashed circles represent visible and eclipsed octahedrally coordinated Li^+ ions. Tetrahedra constructed with solid and chain lines represent respectively occupied and unoccupied Li^+ sites. Arrows in (b) indicate the pathways followed by the interstitial Li^+ ions only.

interstitial Li^+ ions alone this is an example of an interstitialcy mechanism of ion transport. As a result of this interstitialcy mechanism the cluster effectively moves to a neighboring stoichiometric region. At the same time the region initially with the structure of the cluster is converted to a stoichiometric region and vice versa. At the highest temperature, 300°C, a second minority cluster exists; however, the Arrhenius plot (Fig. 5) remains linear throughout the temperature range from 25 to 300°C, suggesting that the dominant cluster of Fig. 2(a) is principally responsible for the ion transport.

$Li_3Zn_{0.5}GeO_4$

Beginning with the solid electrolyte at elevated temperature, 500°C, where the defect structure is relatively simple; the solid solution consists of regions with the structure of the type III cluster and regions of stoichiometric material. The proposed mechanism of Li^+ ion transport is illustrated in Fig. 6; Fig. 6(a) illustrates the structure before migration, 6(b) shows only the pathways followed by the interstitial octahedral Li^+ ions for clarity, and the final structure after migration is shown in 6(c). The net effect is the transport of the defect cluster through the structure. As the temperature is reduced the Arrhenius plot curves downward (Fig. 7). This is accompanied by a change in the defect structure; at these lower temperatures powder neutron diffraction indicates that the Li^+ ions are located in the type I and II clusters. We propose that at these lower
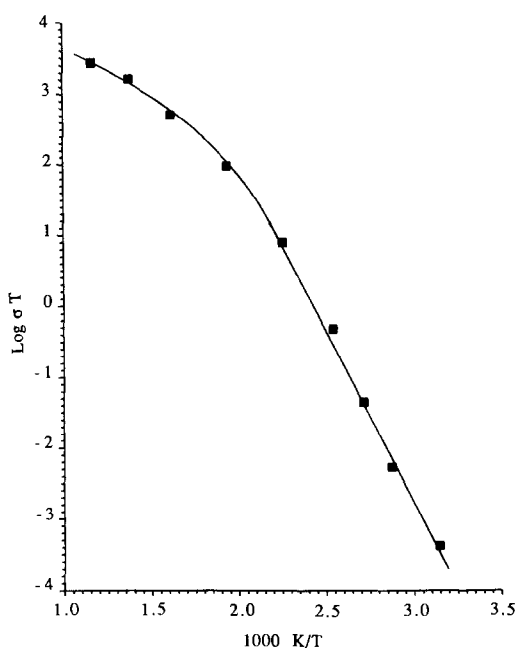
FIG. 7. Arrhenius plot for $Li_3Zn_{0.5}GeO_4$ (σ in Sm^{-1}).

temperatures the type III cluster persists and continues to be the mobile entity, although its concentration is too small to be detected by diffraction techniques. The increased energy required to generate the type III clusters is mainly responsible for the increase in the gradient of the Arrhenius plot at lower temperatures. This behavior is in contrast to the conduction mechanism in $Li_{3.5}Ge_{0.5}V_{0.5}O_4$ in which the mobile defect is dominant throughout the temperature range studied.

General Applicability of the Cluster Model

In simple nonstoichiometric solid electrolytes such as $Ca_{1-x}Y_xF_{2+x}$, the interstitial F^- ions are associated with the immobile Y^{3+} ions because they carry an effective charge of $+1$. The association is strong since the interstitial ion and its charge-compensating defect belong respectively to the anion and cation sublattice; in other words

Y^{3+} and F^- ions are directly bonded near neighbors. Also Y^{3+} is immobile; thus clustering in this system leads to immobilization of interstitial ions. In contrast, interstitial Li^+ ions in $Li_{3+x}Ge_xV_{1-x}O_4$ are compensated by Ge^{4+} ions, and both ions belong to the cation sublattice. The neutron diffraction evidence indicates that the interstitial Li^+ ions are not strongly associated with the Ge^{4+} cations, which carry an effective charge of -1. The Ge^{4+} ions do not appear to exist even as next nearest neighbors to the interstitial Li^+ ions, and there is little evidence of immobilization by the Ge^{4+} cations. Essentially the same model of cluster migration should be applicable to other nonstoichiometric solid electrolytes in which the solid solution mechanism is confined to either the cation or anion sublattice. Theories based on such a cluster mechanism may be capable of explaining the differences in ionic conductivity between different nonstoichiometric solid electrolytes, which is not possible with conventional models involving the motion of randomly distributed ions. The model of cluster migration suggested in this paper bears some similarity to a model proposed much earlier by Van Gool and Bottelberghs (11, 12) in which it is assumed that mobile ions are ordered into domains and that ion transport occurs by domain wall movement. Both models recognize the importance of microscopic ordering in the conduction process.

References

1. M. O'KEEFFE, in "Fast Ion Transport in Solids" (W. van Gool, ed.), North Holland, Amsterdam, 1973.
2. J. B. GOODENOUGH, Proc. R. Soc. London, A 393, 215 (1984).
3. G. E. MURCH AND J. C. DYRE, CRC Crit. Rev Solid State Mater. Sci. 15, 345 (1989).

4. C. R. A. CATLOW, *J. Chem. Soc. Faraday Trans.* **86,** 1167 (1990).

5. A. K. IVANOV-SHITS, N. I. SOROKIN, B. P. SOBOLEV, AND P. P. FEOROV, "International Symposium on Systems with Fast Ionic Transport," p. 99, Dom Techniky, Bratislava, 1985.

6. I. ABRAHAMS, P. G. BRUCE, W. I. F. DAVID, AND A. R. WEST, *Acta Crystallogr. B* **45,** 457 (1989).

7. P. G. BRUCE, I. ABRAHAMS, AND A. R. WEST, *Solid State Ionics* **40/41,** 293 (1990).

8. I. ABRAHAMS AND P. G. BRUCE, *Acta. Crystallogr. B,* in press.

9. P. G. BRUCE AND A. R. WEST, *J. Electrochem. Soc.* **130,** 662 (1983).

10. P. G. BRUCE AND A. R. WEST, *J. Solid State Chem.* **44,** 354 (1982).

11. W. VAN GOOL, *J. Solid State Chem.* **7,** 55 (1973).

12. W. VAN GOOL AND P. H. BOTTELBERGHS, *J. Solid State Chem.* **7,** 59 (1973).